

A highly sensitive, single selective, real-time and “turn-on” fluorescent sensor for Al³⁺ detection in aqueous media†Xiaoyan Shi,^a Huan Wang,^a Tianyu Han,^a Xiao Feng,^a Bin Tong,^{*a} Jianbing Shi,^a Junge Zhi^b and Yuping Dong^{*a}

Received 27th May 2012, Accepted 27th July 2012

DOI: 10.1039/c2jm33393g

A “turn-on” fluorescent sensor, sodium 4,4',4''-(1*H*-pyrrole-1,2,5-triyl)tri-benzoate (Py(PhCOO-Na)₃), has been prepared for the detection of Al³⁺ in aqueous solution. The detection mechanism, as well the mechanism specific to Al³⁺, was studied by fluorescence spectroscopy, UV-vis spectroscopy and dynamic light scattering (DLS) measurement. Py(PhCOONa)₃ exhibited an aggregation-induced emission (AIE) characteristic and was found to show a specific affinity to Al³⁺, as indicated by the enhanced and bathochromically shifted emission of the AIE fluorogen. Upon binding Al³⁺, a significant fluorescence enhancement with a turn-on ratio of over 10-fold was triggered by the AIE process. Moreover, this sensor is highly selective for Al³⁺ over other metal ions with a detection limit of 5 μM and a quantitative detection range of 5–120 μM, and is able to be used in the determination of Al³⁺ in drinking water. The time-response investigation indicates that the emission intensity of (Py(PhCOO⁻)₃) can be quickly boosted to reach the maximum intensity in less than 10 s upon titration of Al³⁺.

Introduction

The molecular design and synthesis of chemosensors to detect metal ions, such as Al³⁺, Hg²⁺, Pb²⁺ and Cu²⁺, has developed rapidly due to the potential impact of their toxic effects. Aluminium ion (Al³⁺) is widely used in food additives, kitchen utensils, packing materials and some Al-based medicines, which increases the risk of Al³⁺ entering into human bodies through the digestive system. It has been found that Al³⁺ ions exerted several neurotoxic effects in organisms a long time ago.¹ For example, Al³⁺ has an important role in Alzheimer's disease, Parkinson's disease, bone softening, chronic renal failure and smoking-related diseases.² Since there is a close association between Al³⁺ and human health, the investigation of Al³⁺ detection attracts more and more attention. In the last decade, several conventional methods have been developed for detecting Al³⁺, including atomic absorption spectrometry, atomic emission spectrometry, inductively coupled plasma mass spectrometry and electrochemical methods.³ These methods, however, require high instrumentation and operation costs and intricate pre-treatment processes. Simple and accurate analytical methods with high

selectivity and sensitivity for the rapid detection of Al³⁺ need to be exploited.

To the best of our knowledge, compared with other metal ions, limited examples of fluorescent or colorimetric chemosensors for the evaluation of Al³⁺ have been reported so far. Their signal transduction is generally achieved by photoinduced electron transfer, photoinduced charge-transfer, Förster resonance energy transfer, or switching on of Au–Au interactions.⁴ The majority of these methods have limitations such as weakness in their selectivity and sensitivity over other metal cations, tedious synthetic efforts and/or a lack of practical applicability in aqueous solution. Thus, it is desirable to develop novel methods for the selective detecting of Al³⁺ ions in aqueous environments.

Tang's group in 2001 first reported that the luminescence of silole molecules is stronger in the aggregated state than that in the solution state.⁵ A variety of luminogens, including distyrylbenzene, fluorene, pentacene and pyrene derivatives, were successively proved to have the same properties.⁶ These molecules can be generally categorized into two groups. In the first group, the luminogenic molecules are non-emissive when dissolved in good solvents but become highly luminescent when aggregated in the solid state, thus behaving exactly oppositely to the conventional ACQ luminophores. Since the emission is induced by aggregation, Tang coined “aggregation-induced emission” (AIE) for this unusual phenomenon.⁵ In the second group, the luminogens are luminescent in solution and become more emissive in the aggregated state. Because the light emission is enhanced by aggregate formation, the effect is referred to as

^aCollege of Materials Science and Engineering, Beijing Institute of Technology, 5 South Zhongguancun Street, Beijing, 100081, China. E-mail: tongbin@bit.edu.cn; chdongyp@bit.edu.cn; Fax: +86 10-68948982

^bCollege of Chemistry, Beijing Institute of Technology, 5 South Zhongguancun Street, Beijing, 100081, China

† Electronic supplementary information (ESI) available: See DOI: 10.1039/c2jm33393g

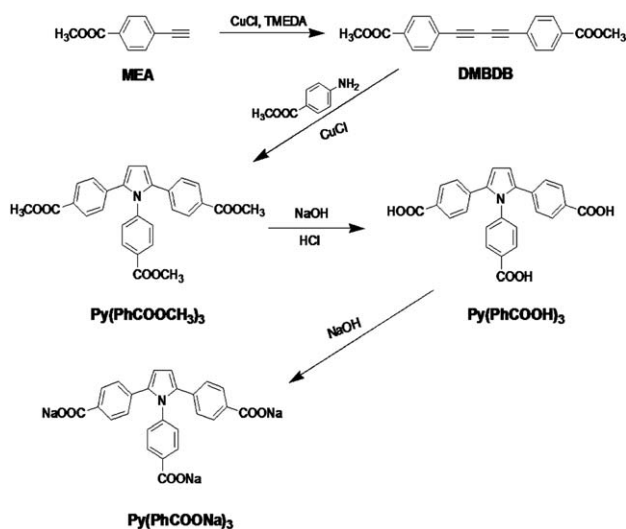
“aggregation-induced emission enhancement” (AIEE).⁷ Such a novel effect has enabled the AIE(E) luminogens to find potential high-tech applications in sensors and opto-electrical devices over the past years.^{5–8} Above all, the introduction of functional groups into AIE(E) molecules will favor the new development of chemor biosensors for detecting metal cations, biomolecules, organic vapors, chiral molecules and explosives.⁹

In our previous research, we found that 1,2,5-triphenylpyrrole (TPP) derivatives exhibited good AIEE properties. Especially, sodium 4-(2,5-diphenyl-1*H*-pyrrol-1-yl)benzoate (TriPP-COONa), with one carboxylate group in TPP, can form highly fluorescent aggregates with aluminium and has been used for selective and sensitive detecting Al³⁺ in THF–water mixtures (25 : 75, v/v) based on the AIE mechanism.¹⁰ Herein, to further improve the water solubility of TPP derivatives and thus to realize the detection of metal ions in aqueous media, we synthesized a new TPP derivative, sodium 4,4',4''-(1*H*-pyrrole-1,2,5-triyl)tribenzoate (Py(PhCOONa)₃), and explored their utility as metal ion sensors on the basis of its AIE characteristic. Py(PhCOONa)₃ was proved to be a highly sensitive, singly selective, real-time and “turn-on” fluorescence sensor for Al³⁺ in aqueous media.

Results and discussion

Synthesis and characterization of Py(PhCOONa)₃

The general synthetic procedure is shown in Scheme 1. Dimethyl 4,4'-(buta-1,3-diyne-1,4-diyl)dibenzoate (DMBDB) was synthesized from starting material methyl 4-ethynylbenzoate (MEA) by the Glaser coupling reaction. The Schulte–Reisch reaction of DMBDB with methyl 4-aminobenzoate gave the corresponding trimethyl 4,4',4''-(1*H*-pyrrole-1,2,5-triyl)tribenzoate (Py(PhCOOCH₃)₃). Hydrolysis of Py(PhCOOCH₃)₃ to produce 4,4',4''-(1*H*-pyrrole-1,2,5-triyl)tribenzoic acid (Py(PhCOOH)₃) followed by neutralization with sodium hydroxide afforded sodium 4,4',4''-(1*H*-pyrrole-1,2,5-triyl)tribenzoate (Py(PhCOONa)₃) in a good yield.



Scheme 1 Synthesis route to Py(PhCOONa)₃.

All the compounds were characterized by ¹H-NMR, infrared spectroscopy (IR), and matrix-assisted laser desorption/ionization time of flight mass spectrometry (MALDI-TOF MS). For instance, two peaks at $\delta = 6.63$ ppm and $\delta = 3.94$ ppm attributed to the pyrrole moiety and ester groups, respectively, are clearly observed for Py(PhCOOCH₃)₃ in the ¹H-NMR spectra (Fig. S1 in the ESI†). The disappearance of the peak at $\delta = 3.94$ ppm corresponded to the ester groups, as well as the appearance of a new peak at $\delta = 13.01$ ppm attributed to the carboxyl groups, demonstrates that Py(PhCOOCH₃)₃ underwent a complete hydrolysis and was entirely converted to Py(PhCOOH)₃. The IR spectra of Py(PhCOOCH₃)₃ and Py(PhCOOH)₃ displayed middle peaks in the 1724–1680 cm⁻¹ region that are characteristics of the C=O stretching vibration of carbonyl. Compared to the IR spectrum of Py(PhCOOCH₃)₃, the appearance of a broad band in the range 3590–2680 cm⁻¹ is indicative of the existence of carboxyl groups of Py(PhCOOH)₃. Meanwhile, the two signals around 1400 and 1600 cm⁻¹ in the IR spectrum of Py(PhCOONa)₃ are assigned to the symmetrical and anti-symmetrical vibration of –COO⁻, respectively. In addition, in the 1600–1430 cm⁻¹ region, the transmission bands are in accordance with the skeletal vibrations of aromatic and heterocyclic rings for all these three compounds (Fig. S2 in the ESI†). The MS data of Py(PhCOOCH₃)₃ and Py(PhCOOH)₃ tally with the theoretical ones (Fig. S3 in the ESI†).

Aggregation-induced emission

Py(PhCOONa)₃ exhibits good solubility in water. The dilute aqueous solution of Py(PhCOONa)₃ hardly shows any fluorescence (fluorescence quantum yield, 0.003%) as shown in Fig. 1 and 2. Because THF is a poor solvent for it, Py(PhCOO⁻)₃ must have aggregated in the H₂O–THF mixture. To investigate the AIE property of Py(PhCOO⁻)₃, the fluorescence behaviour of the H₂O–THF mixtures in different ratios was examined at the same Py(PhCOO⁻)₃ concentration under identical measurement conditions. The fluorescence spectrum of Py(PhCOO⁻)₃ (10 μM) exhibits an emission band at 413 nm in H₂O–THF (5 : 95, v/v) mixture when excited at 328 nm. As THF content increased from

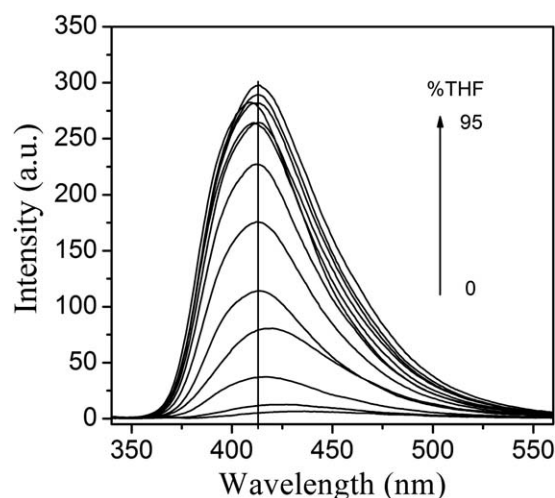


Fig. 1 Emission spectra of Py(PhCOO⁻)₃ (10 μM) in H₂O–THF mixture with different THF contents. Excitation wavelength: 340 nm.

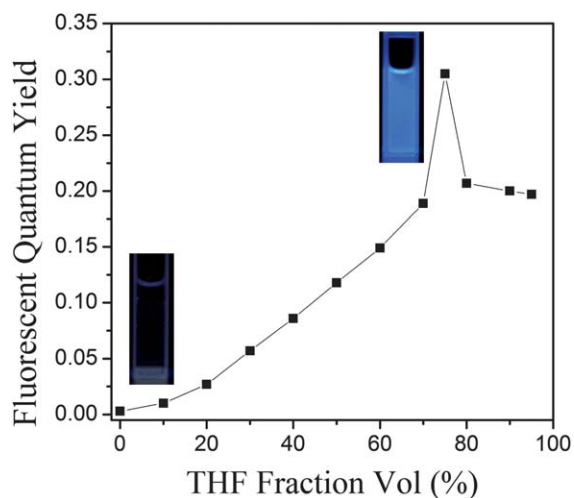


Fig. 2 Fluorescent quantum yield of $\text{Py}(\text{PhCOO}^-)_3$ vs. composition of H_2O -THF mixture. Quinine sulfate in 0.1 M H_2SO_4 was used as reference.

0% to 95%, the photoluminescence (PL) intensities and fluorescent quantum yield were dramatically enhanced (Fig. 1 and 2, and Fig. S4 in the ESI[†]). Even in the H_2O -THF (90/10, v/v) mixture, the fluorescence was still much higher than that in pure water. The photoluminescence (PL) emission, however, reached the maximum value at 75% THF content. The decrement of fluorescent quantum yield and PL intensity along with the THF content from 75% to 95% was probably due to the quick agglomeration of the $\text{Py}(\text{PhCOO}^-)_3$ molecules in a random way, which forms less emissive, “redder”, amorphous powders.^{6b-d}

It's wholly different from TriPPCOO^- whose emission intensities almost remained in nullity at “low” THF fraction content (<40%) and only showed an uprush at much higher THF contents (>40%).^{10b} The enhancement in luminescence, after the addition of nonsolvent, resulted from the changing of the existing forms (the relative distance between the molecules and geometry of compounds in the solution state) from a solution state in water to the aggregated particles in the H_2O -THF mixture. That is, the emission of $\text{Py}(\text{PhCOO}^-)_3$ is spectacularly boosted by aggregation, in other words, $\text{Py}(\text{PhCOO}^-)_3$ is AIE active. Since the solubility of $\text{Py}(\text{PhCOONa})_3$ with three charged carboxylate groups in THF is much lower than that of TriPPCOONa , that is, the formation of $\text{Py}(\text{PhCOO}^-)_3$ aggregates is easier than that of TriPPCOO^- in the presence of THF, it will provide more possibilities of detecting metal ions in aqueous solution with lower THF content.

Fluorogenic Al^{3+} sensing

Given the fact that $\text{Py}(\text{PhCOO}^-)_3$ has already existed in an aggregated form in H_2O -THF (96/4, v/v) mixtures, one can expect that the introduction of Al^{3+} into $\text{Py}(\text{PhCOO}^-)_3$ solution would lead to the formation of $\text{Py}(\text{PhCOO}^-)_3\text{-nAl}^{3+}$ ($n = 1, 2$ or 3) salts with lower solubility. As a result of increasing the aggregation degree, a “turn-on” fluorescent signal could be detected based on the AIE mechanism. The emission spectra of 100 μM $\text{Py}(\text{PhCOO}^-)_3$ in H_2O -THF (96/4, v/v) mixture upon titration with Al^{3+} are shown in Fig. 3. With increasing Al^{3+}

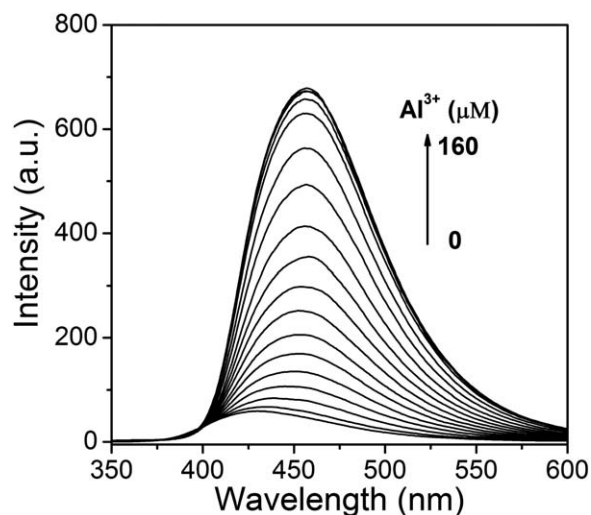


Fig. 3 Emission spectra of $\text{Py}(\text{PhCOO}^-)_3$ (100 μM) in H_2O -THF (96/4, v/v) mixture upon addition of Al^{3+} . The Al^{3+} concentrations are 0, 10, 20, 30...160 μM , from bottom to top.

concentration from 0 to 170 μM , the emission band at 428 nm showed a steady and smooth enhancement and red-shift when excited at 328 nm. A “turn-on” ratio over 10-fold was triggered with the addition of 1.6 equiv. of Al^{3+} . Fig. 4 shows the dependence of the changes in emission intensity on the Al^{3+} concentration. It exhibited a three-phase increment upon the increasing of Al^{3+} concentration, a slow growth before 50 μM , a rapid growth in the range of 50–130 μM , and a suspended manner afterward. Notably, there exists a good linear relationship between the changes in PL intensity and the square of Al^{3+} concentration ($R^2 = 0.9979$, 0–130 μM). Its quantitative detection range is much more broader than that of TriPPCOO^- ,^{10b}

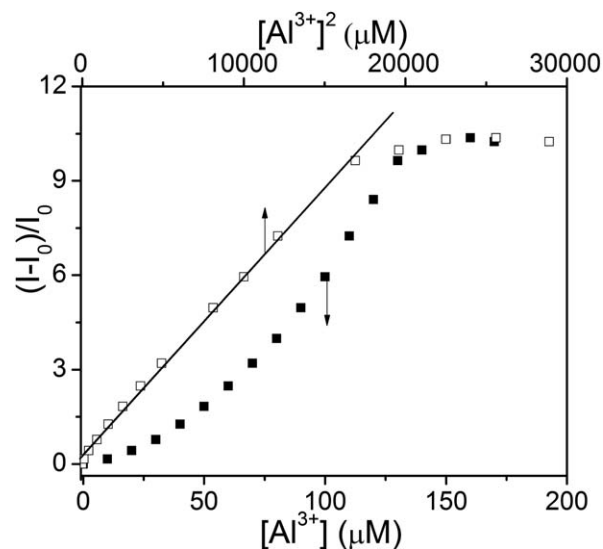


Fig. 4 Emission intensities of $\text{Py}(\text{PhCOO}^-)_3$ (100 μM) in H_2O -THF mixture (96/4, v/v) as a function of $[\text{Al}^{3+}]$ or $[\text{Al}^{3+}]^2$ (0–170 μM). Excitation wavelength: 340 nm. Inset: Linear relationship between emission growth ratio and Al^{3+} concentration from 0 μM to 130 μM . Curve-fit equation: $(I - I_0)/I_0 = 0.27809 + 5.67207 \times 10^{-4} [\text{Al}^{3+}]^2$, $R^2 = 0.99786$.

indicating that this approach is more applicable for quantitative detection of Al^{3+} . In addition, the detection limit of $\text{Py}(\text{PhCOO}^-)_3$ towards Al^{3+} was estimated as $5.3 \mu\text{M}$, which meets the limit for drinking water according to the WHO standard ($7.41 \mu\text{M}$).

To further evaluate the specificity of $\text{Py}(\text{PhCOONa})_3$ towards Al^{3+} , we carried out fluorescence titration with other cations, including Al^{3+} , $\text{N}(\text{CH}_3)_4^+$, Au^{3+} , Cr^{2+} , Ni^{2+} , Cd^{2+} , Hg^{2+} , Fe^{3+} , Pb^{2+} , Ag^+ , Ce^{2+} , Cu^{2+} , Zn^{2+} , Ba^{2+} , Mg^{2+} , Ca^{2+} and K^+ , at concentrations of $500 \mu\text{M}$ to make sure of its maximum fluorescent response. Although $\text{Py}(\text{PhCOO}^-)_3$ has a positive response towards Au^{3+} , Cr^{2+} , Pb^{2+} and Cu^{2+} , as well as a negative response toward Hg^{2+} , Fe^{3+} and Ag^+ , it is clearly seen that the most striking effects are observed for Al^{3+} , confirming the probe is selectively responsive to Al^{3+} (Fig. 5). Compared with the detection result in pure water, the ratio of H_2O and THF (96/4, v/v) used in the sensory experiments was chosen according to its relatively higher selectivity and stronger amplification ability owing to the formation of $\text{Py}(\text{PhCOO}^-)_3$ AIE aggregates induced by THF (Fig. 5). Compared with TriPPCOO^- , $\text{Py}(\text{PhCOO}^-)_3$ exhibits improved selectivity due to its relative higher solubility and COO^- density. To further testify single selectivity of $\text{Py}(\text{PhCOO}^-)_3$ for Al^{3+} in practical application, we chose K^+ , Mg^{2+} , Ca^{2+} , and Ba^{2+} ions as the interfering ions, some of which have a relatively high concentration in biological tissue and drinking water. As shown in Fig. 5, the experimental results indicated that fluorescent intensities of $\text{Py}(\text{PhCOO}^-)_3$ at 460 nm enhanced by Al^{3+} aren't much affected by the existence of the interfering ions, thus providing a potential application for biological detection and water quality monitoring.

Moreover, ion recognition properties of $\text{Py}(\text{PhCOO}^-)_3$ have also been studied by using an absorption technique. The UV-vis spectra of $\text{Py}(\text{PhCOO}^-)_3$ in water-THF (96/4, v/v) mixtures showed only one $\pi-\pi^*$ transition band centered at 329 nm , which can be assigned to the aryl-substituted pyrrole moiety

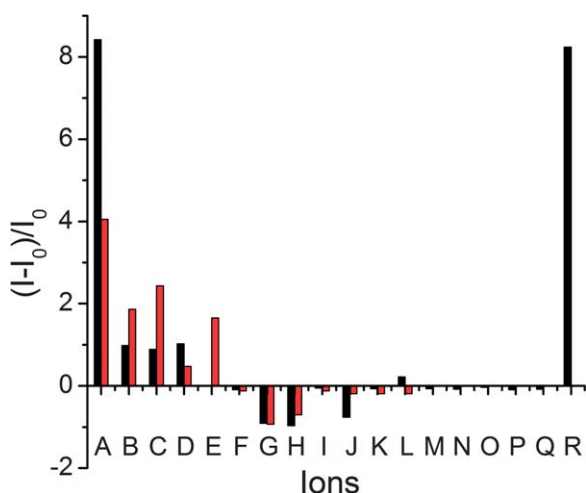


Fig. 5 The maximum fluorescent response of $\text{Py}(\text{PhCOO}^-)_3$ ($100 \mu\text{M}$) upon addition of different metal ions ($500 \mu\text{M}$) in H_2O -THF (96/4, v/v) mixtures (black columns) or pure water (red columns), listed from left to right: (A) Al^{3+} , (B) $\text{N}(\text{CH}_3)_4^+$, (C) Au^{3+} , (D) Cr^{2+} , (E) Ni^{2+} , (F) Cd^{2+} , (G) Hg^{2+} , (H) Fe^{3+} , (I) Pb^{2+} , (J) Ag^+ , (K) Ce^{2+} , (L) Cu^{2+} , (L) Zn^{2+} , (N) Ba^{2+} , (O) Mg^{2+} , (P) Ca^{2+} , (Q) K^+ , and (R) $\text{Al}^{3+} + \text{Ba}^{2+} + \text{Mg}^{2+} + \text{Ca}^{2+} + \text{K}^+$.

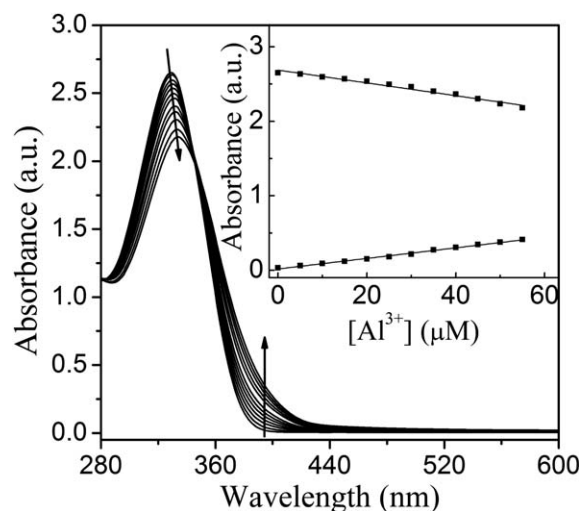


Fig. 6 Absorption response of $\text{Py}(\text{PhCOO}^-)_3$ ($100 \mu\text{M}$) to the titration of Al^{3+} in H_2O -THF (96/4, v/v) mixture. The $[\text{Al}^{3+}]$ total increases from 0 to $60 \mu\text{M}$ along the direction of the arrow. Inset: Linear relationship between absorbance and Al^{3+} concentration at 329 and 391 nm .

(Fig. 6). Upon addition of Al^{3+} (0 - $60 \mu\text{M}$), the absorbance at 329 nm decreased gradually with slight red-shift while the absorbance at 346 nm remained constant along with the increase of the Al^{3+} concentration. In the meanwhile, although a new absorption band was not obviously observed, a low energy (LE) shoulder developed at 391 nm (Fig. 6). The presence of a well-defined isosbestic point at 346 nm indicated that interconversion between the uncomplexed and complexed species had occurred. Besides, the transmittance of the solution decreased upon titration with Al^{3+} and reached its minimum value when the Al^{3+} concentration was over $200 \mu\text{M}$ (Fig. S5 in the ESI†), which implies the amount of aggregates became larger and/or the size of aggregates became bigger with increasing the Al^{3+} content. These assumptions were further confirmed by dynamic light scattering (DLS) measurement. The average particle size of $\text{Py}(\text{PhCOO}^-)_3$

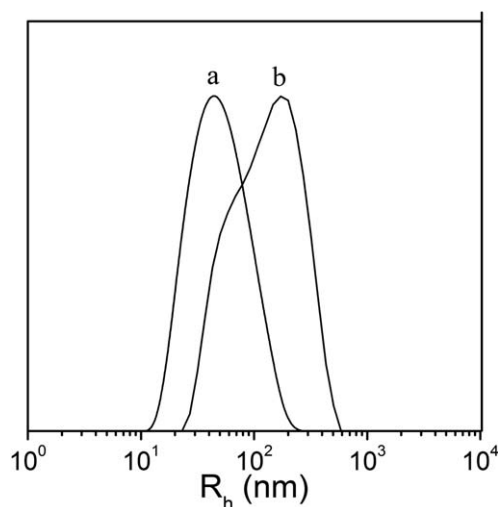


Fig. 7 Particle size distribution in $\text{Py}(\text{PhCOO}^-)_3$ ($100 \mu\text{M}$, H_2O -THF 96/4, v/v) solution with (b) and without (a) the addition of Al^{3+} ($500 \mu\text{M}$) determined by DLS.

in H₂O–THF (96/4, v/v) solution increased from 50 to 130 nm upon addition of Al³⁺ (500 μM) (Fig. 7). Thus, an AIE mechanism is contributed to the ‘turn-on’ detection of Py(PhCOO⁻)₃ for Al³⁺ herein.

In order to elucidate the effect of Al³⁺ on aggregate formation, the morphology of Py(PhCOO⁻)₃ aggregates in H₂O–THF (96/4, v/v) mixtures without and with Al³⁺ was examined by transmission electron microscopy (TEM). The TEM image of the sample without Al³⁺ showed the amorphous and incompact aggregates because of the electrostatic repulsion between carboxylate ions (Fig. 8a). The diameters of the approximative spheres ranged from 15 to 100 nm with a 45.3 nm average diameter, which is consistent with that from DLS analysis (Fig. 7, line a). Part of the nanospheres further clumped together to form nanoclusters with random morphologies. In the Al³⁺-containing sample, the TEM image, however, revealed that the introduction of Al³⁺ leads to the morphological transition of aggregates in H₂O–THF (96/4, v/v) mixtures. Aggregates composed of spheres, capsules and ribbons were observed (Fig. 8). Especially, the morphology of spheres and capsules is more regular and more compact than that of Py(PhCOO⁻)₃ aggregates in H₂O–THF (96/4, v/v) mixtures without Al³⁺, which indicates that the introduction of Al³⁺ promotes Py(PhCOO⁻)₃ to form regular aggregates. The diameters of the spheres and capsules ranges from 23 to 71 nm with a 47 nm average diameter. For the ribbons, their average width and length are about 30 and 120 nm, respectively. The results also explain the corresponding attributions of the two peaks showed in Fig. 7, line b. According to previous studies, reducing the anionic repulsion between Al³⁺ and amphiphilic Py(PhCOO⁻)₃ headgroups enables closer packing to fabricate spheres and can provide an additional impetus for capsule formation.¹¹ Because the concentration of Al³⁺ was much higher than that of Py(PhCOO⁻)₃ herein, the decrease in charge of partial unilamellar vesicle bilayers could, in turn, induce the stacks of lamellae to form the ribbons by decreasing the repulsive force between anionic bilayers.¹²

Time response of Py(PhCOO⁻)₃ to Al³⁺

The time-dependent fluorescence intensity of H₂O–THF (96/4, v/v) solution of Py(PhCOO⁻)₃ to Al³⁺ was evaluated. Because the minimum response time that can be measured is limited in the manipulation time, all the measurements with different Al³⁺ contents were started at 10 s. As shown in Fig. 9 and S6 in the ESI,[†] the emission intensity was immediately enhanced up to the

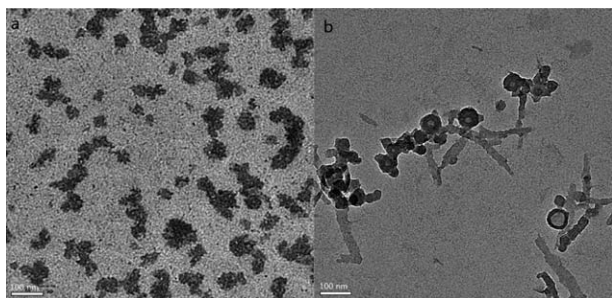


Fig. 8 TEM images of the Py(PhCOO⁻)₃ (100 μM) in H₂O–THF (96/4, v/v) mixture (a) without and (b) with 500 μM Al³⁺.

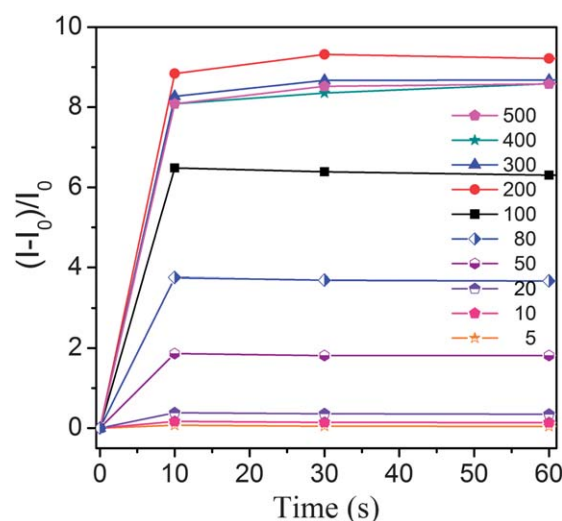
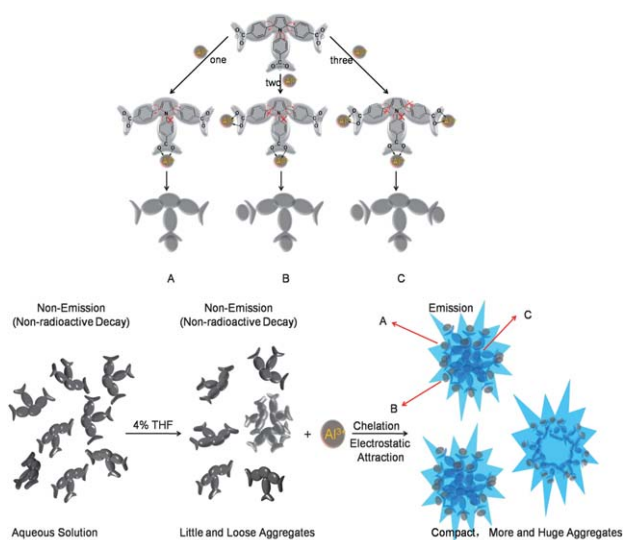


Fig. 9 Fluorescence response of Al³⁺ with different concentrations (5–500 μM) at different times.

maximum after the addition of Al³⁺ in a few seconds and stays invariable over an extended period of time. This performance is much faster than that of TriPPCOO⁻ reported by our group, which increased to the maximum in 300 s.^{10b} We compared this phenomenon to that attributed with the TriPPCOO⁻ aggregates, and there are more carboxylate groups that could bind with Al³⁺ through electrostatic attractions existing on the surface of Py(PhCOO⁻)₃ aggregates. This provides a potential ‘zero-wait’ detecting method for Al³⁺.

Response mechanism of Py(PhCOO⁻)₃ to Al³⁺

We supposed that the fluorescence enhancement after addition of Al³⁺ is assigned to a synergetic effect based on the AIE mechanism. On one hand, according to literature, both the experimental results and the theoretical calculations have revealed that the bidentate complex formed between carboxylate groups and Al³⁺ is more stable than the mono-dentate complex.¹³ When one carboxylate group in Py(PhCOO⁻)₃ is used to form a bidentate complex with Al³⁺ ion, the pyrrole ring easily constructs the coplanar conformation with the benzyl ring, which further favours the aggregation and suppresses intramolecular-rotation causes non-radiative decay, that is, an AIE mechanism (Scheme 2). Thus, the PL intensity of Py(PhCOO⁻)₃ is enhanced with the increasing of Al³⁺ concentration. On the other hand, little and loose aggregates are considered to be formed in the initial Py(PhCOO⁻)₃ (100 μM, THF/water, 96/4, v/v) solution, which can be proved by the DLS data and TEM images (Fig. 7 and 8). Owing to its small size, high charge density and oxophilicity, Al³⁺ will immediately get close to carboxylate groups existing on the surface of these aggregates and then form a chelation complex with lower solubility through electrostatic attractions. This can not only increase the amount and the size of the aggregates but also compact them. All these impacts can suppress intramolecular-rotation, cause non-radiative decay and boost the fluorescence emission based on the AIE mechanism (Scheme 2).



Scheme 2 The sensing process based on the AIE mechanism.

Experimental section

All chemicals were purchased from Alfa Aesar and Beijing Chemical Reagent Company without further purification. Solvents were purified according to standard procedures. The structures of the products synthesized in this paper were identified by $^1\text{H-NMR}$ spectra, elemental analysis and mass spectra through Bruker ARX-400 spectrometer, Elementar Vario EL and Autoflex III MALDI-TOF, respectively. UV-visible absorption spectra were measured by TU-1901 spectrophotometer. The emission spectra were carried out on a Perkin-Elmer VARIAN 55 spectrophotometer. Particle size distribution analysis was determined by an ALV-5000 dynamic laser light scattering. Samples were examined in a Tecnai Spirit 120 kV transmission electron microscope. The TEM was operated at 80 kV accelerating potential. The samples were prepared as following steps: the solutions of $\text{Py}(\text{PhCOO}^-)_3$ (100 μM) without (as blank) or with 500 μM Al^{3+} in $\text{H}_2\text{O-THF}$ (96/4 v/v) mixture were absorbed onto copper mesh for 1 minute and dried at ambient temperature, then they were washed with pure water. In addition, the blank was re-dyed with uranyl acetate for 30 seconds.

$\text{Py}(\text{PhCOOCH}_3)_3$: compound 1,4-di(4-(methoxycarbonyl)phenyl)buta-1,3-diyne was synthesized according to our previous work.^{10b} A mixture of 1,4-di(4-(Methoxycarbonyl)phenyl)buta-1,3-diyne (20.0 mmol), copper(i) chloride (2.0 mmol), and methyl 4-aminobenzoate (30.0 mmol) was stirred under argon for 12 h at 170 $^\circ\text{C}$. The crude product was purified by column chromatography (ethyl acetate/petroleum ether (the boiling range: 30–60 $^\circ\text{C}$) 7 : 1), and then recrystallized from chloroform and *n*-hexane, yield: 32.8%. $^1\text{H NMR}$ (400 MHz, CDCl_3) δ (ppm): 7.98–7.96 (d, 2H), 7.88–7.86 (d, 4H), 7.11–7.09 (d, 6H), 6.63 (s, 2H), 3.94–3.91 (d, 9H). Anal. calcd for $\text{C}_{28}\text{H}_{23}\text{NO}_6$: C 71.63, H 4.94, N 2.98; found: C 71.29, H 4.96, N 2.93%. MS (MALDI-TOF): calcd for $\text{C}_{28}\text{H}_{23}\text{NO}_6$, 469.15; found, 469.0.

$\text{Py}(\text{PhCOOH})_3$: $\text{Py}(\text{PhCOOCH}_3)_3$ (0.8 mmol) in 100 mL and 50 mL of H_2O in which dissolved NaOH (5 mmol) was added into a 250 mL round bottom flask, then the mixture was stirred at

70 $^\circ\text{C}$ for 15.5 h and poured into 500 mL dilute hydrochloric acid solution, the white precipitate was washed by H_2O , ethanol and dichloromethane several times, yield: 87.6%. $^1\text{H NMR}$ (400 MHz, DMSO) δ (ppm): 13.01 (s, 3H), 7.92–7.90 (d, 2H), 7.76 (s, 4H), 7.22–7.11 (m, 6H), 6.70 (s, 2H). MS (MALDI-TOF): calcd for $\text{C}_{25}\text{H}_{17}\text{NO}_6$, 427.11; found, 426.9.

$\text{Py}(\text{PhCOONa})_3$: $\text{Py}(\text{PhCOOH})_3$ (0.05 mmol) was neutralized with aqueous sodium hydroxidesolution (0.15 mmol), stirred overnight and then $\text{Py}(\text{PhCOONa})_3$ was afforded after the drying process. $^1\text{H NMR}$ (400 MHz, D_2O) δ (ppm): 7.72–7.57 (m, 6H), 7.07–7.03 (m, 6H), 6.58 (s, 2H).

Conclusions

In summary, a singly selective and highly sensitive water-soluble probe for the real-time and “turn-on” detection of Al^{3+} was synthesized by the introduction of three carboxylate functional groups into the aryl-substituted pyrrole derivative. The complexation of Al^{3+} with $\text{Py}(\text{PhCOO}^-)_3$ triggered a significant enhancement of fluorescence intensity in aqueous solution based on the AIE mechanism. We suppose that the selectivity is probably due to the difference of the electrostatic binding ability between metal ions and $-\text{COO}^-$ as well as the solubility of the complex. Such a real-time detection method in aqueous solution based on AIE mechanism has a huge prospect of application in chemosensing and biosensing fields. Further studies on the design of novel fluorescent probes for metal ions with this principle are underway.

Acknowledgements

The authors are grateful to the National Natural Scientific Foundation of China (Grant nos. 20634020, 51073026, 51061160500, 20944004, 21074011), the Specialized Research Fund for the Doctoral Program of Higher Education of China (Grant nos. 20091101110031 and 20101101120029), Basic Research Foundation of Beijing Institute of Technology, Excellent Young Scholars Research Fund of Beijing Institute of Technology (Grant no. 2009Y0914), Technology Innovation Programme for Graduate Students of Beijing Institute of Technology (Grant no. 2011cx03032) for financial support of this work.

Notes and references

- (a) R. A. Yokel, *Fundam. Appl. Toxicol.*, 1987, **9**, 795–806; (b) V. Bernuzzi, D. Desorand and P. R. Lehr, *Teratology*, 1989, **40**, 21–27; (c) G. Muller, V. Bernuzzi, D. Desor, M. F. Hutin, D. Burnel and P. R. Lehr, *Teratology*, 1990, **42**, 253–261; (d) J. M. Donald, M. S. Golub, M. E. Gershwin and C. L. Keen, *Neurotoxicol. Teratol.*, 1989, **11**, 345–351; (e) M. S. Golub, M. E. Gershwin, J. M. Donald, S. Negri and C. L. Keen, *Fundam. Appl. Toxicol.*, 1987, **8**, 346–357.
- (a) D. R. Crapper, S. S. Krishnan and A. J. Dalton, *Science*, 1973, **180**, 511–513; (b) D. P. Perl and A. R. Brody, *Science*, 1980, **208**, 297–299; (c) D. P. Perl, D. C. Gajdusek, R. M. Garruto, R. T. Yanagihara and C. J. Gibbs, *Science*, 1982, **217**, 1053–1055; (d) E. House, J. Collingwood, A. Khan, O. Korchazkina, G. Berthon and C. Exley, *J. Alzheimer's Dis.*, 2004, **6**, 291–301; (e) T. P. Flaten, *Brain Res. Bull.*, 2001, **55**, 187–196; (f) C. Exley, *J. Alzheimer's Dis.*, 2006, **10**, 173–177; (g) C. Exley, *J. Alzheimer's Dis.*, 2006, **10**, 451–452; (h) C. Exley, A. Begum, M. P. Woolley and R. N. Bloor, *Am. J. Med.*, 2006, **119**, 276; (i) C. Exley, *J.*

- Alzheimer's Dis.*, 2007, **12**, 313–318; (j) E. House, M. Esiri, G. Forster, P. G. Ince and C. Exley, *Metallomics*, 2012, **4**, 56–65.
- 3 (a) T. F. Guray, Ü. D. Uysal, T. Gedikbey and A. A. Huseyinli, *Anal. Chim. Acta*, 2005, **545**, 107–112; (b) I. Narin, M. Tuzen and M. Soyak, *Talanta*, 2004, **63**, 411–418; (c) H. M. Wang, Z. L. Yu, Z. L. Wang, H. J. Hao, Y. M. Chen and P. Y. Wan, *Electroanalysis*, 2011, **23**, 1095–1099; (d) X. J. Xie and Y. Qin, *Sens. Actuators, B*, 2011, **156**, 213–217.
- 4 (a) S. H. Kim, H. S. Choi, J. Kim, S. J. Lee, D. T. Quang and J. S. Kim, *Org. Lett.*, 2010, **12**, 560–563; (b) Y. W. Wang, M. X. Yu, Y. H. Yu, Z. P. Bai, Z. Shen, F. Y. Li and X. Z. You, *Tetrahedron Lett.*, 2009, **50**, 6169–6172; (c) A. Ben Othman, J. W. Lee, Y. D. Huh, R. Abidi, J. S. Kim and J. Vicens, *Tetrahedron*, 2007, **63**, 10793–10800; (d) D. Maity and T. Govindaraju, *Chem. Commun.*, 2010, **46**, 4499–4501; (e) M. Arduini, F. Felluga, F. Mancini, P. Rossi, P. Tecilla, U. Tonellato and N. Valentinuzzi, *Chem. Commun.*, 2003, 1606–1607; (f) J. L. Ren, J. Zhang, J. Q. Luo, X. K. Pei and Z. X. Jiang, *Analyst*, 2001, **126**, 698–702; (g) J. Q. Wang, L. Huang, L. Gao, J. H. Zhu, Y. Wang, X. X. Fan and Z. G. Zou, *Inorg. Chem. Commun.*, 2008, **11**, 203–206; (h) F. K. Hau, X. M. He, W. H. Lam and V. W. W. Yam, *Chem. Commun.*, 2011, **47**, 8778–8780.
- 5 J. D. Luo, Z. L. Xie, J. W. Y. Lam, L. Cheng, H. Y. Chen, C. F. Qiu, H. S. Kwok, X. W. Zhan, Y. Q. Liu, D. B. Zhu and B. Z. Tang, *Chem. Commun.*, 2001, 1740–1741.
- 6 (a) J. W. Chen, C. C. W. Law, J. W. Y. Lam, Y. P. Dong, S. M. F. Lo, I. D. Williams, D. B. Zhu and B. Z. Tang, *Chem. Mater.*, 2003, **15**, 1535–1546; (b) H. Tong, Y. Dong, M. Haussler, J. W. Y. Lam, H. H.-Y. Sung, I. D. Williams, J. Sun and B. Z. Tang, *Chem. Commun.*, 2006, 1133–1135; (c) Y. Q. Dong, J. W. Y. Lam, A. J. Qin, Z. Li, J. Z. Sun, H. H. Y. Sung, I. D. Williams and B. Z. Tang, *Chem. Commun.*, 2007, 40–42; (d) Y. Q. Dong, J. W. Y. Lam, A. J. Qin, J. X. Sun, J. Z. Liu, Z. Li, J. Z. Sun, H. H. Y. Sung, I. D. Williams, H. S. Kwok and B. Z. Tang, *Chem. Commun.*, 2007, 3255–3257; (e) Z. Li, Y. Dong, B. X. Mi, Y. H. Tang, M. Haussler, H. Tong, Y. P. Dong, J. W. Y. Lam, Y. Ren, H. H. Y. Sung, K. S. Wong, P. Gao, I. D. Williams, H. S. Kwok and B. Z. Tang, *J. Phys. Chem. B*, 2005, **109**, 10061–10066; (f) G. Yu, S. W. Yin, Y. Q. Liu, J. S. Chen, X. J. Xu, X. B. Sun, D. G. Ma, X. W. Zhan, Q. Peng, Z. G. Shuai, B. Z. Tang, D. B. Zhu, W. H. Fang and Y. Luo, *J. Am. Chem. Soc.*, 2005, **127**, 6335–6346; (g) Y. Liu, X. T. Tao, F. Z. Wang, X. N. Dang, D. C. Zou, Y. Renan and M. H. Jiang, *J. Phys. Chem. C*, 2008, **112**, 3975–3981; (h) H. G. Lu, B. Xu, Y. J. Dong, F. P. Chen, Y. W. Li, Z. F. Li, J. T. He, H. Li and W. J. Tian, *Langmuir*, 2010, **26**, 6838–6844.
- 7 (a) Q. Zeng, Z. Li, Y. Dong, C. Di, A. Qin, Y. Hong, L. Ji, Z. Zhu, C. K. W. Jim, G. Yu, Q. Li, Z. Li, Y. Liu, J. Qin and B. Z. Tang, *Chem. Commun.*, 2007, 70–72; (b) K. Y. Pu and B. Liu, *Adv. Funct. Mater.*, 2009, **19**, 277–284; (c) K. Y. Pu, L. P. Cai and B. Liu, *Macromolecules*, 2009, **42**, 5933–5940; (d) K. Y. Pu and B. Liu, *J. Phys. Chem. B*, 2010, **114**, 3077–3084; (e) W. Z. Yuan, H. Zhao, X. Y. Shen, F. Mahtab, J. W. Y. Lam, J. Z. Sun and B. Z. Tang, *Macromolecules*, 2009, **42**, 9400–9411; (f) A. J. Qin, J. W. Y. Lam, L. Tang, C. K. W. Jim, H. Zhao, J. Z. Sun and B. Z. Tang, *Macromolecules*, 2009, **42**, 1421–1424; (g) K. Kokado, A. Nagai and Y. Chujo, *Macromolecules*, 2010, **43**, 6463–6468; (h) J. Z. Liu, Y. C. Zhong, J. W. Y. Lam, P. Lu, Y. N. Hong, Y. Yu, Y. N. Yue, M. Faisal, H. H. Y. Sung, I. D. Williams, K. S. Wong and B. Z. Tang, *Macromolecules*, 2010, **43**, 4921–4936.
- 8 (a) M. Wang, X. G. Gu, G. X. Zhang, D. Q. Zhang and D. B. Zhu, *Anal. Chem.*, 2009, **81**, 4444–4449; (b) L. Liu, G. X. Zhang, J. F. Xiang, D. Q. Zhang and D. B. Zhu, *Org. Lett.*, 2008, **10**, 4581–4584; (c) Y. N. Hong, S. J. Chen, C. W. T. Leung, J. W. Y. Lam, J. Z. Liu, N. W. Tseng, R. T. K. Kwok, Y. Yu, Z. K. Wang and B. Z. Tang, *ACS Appl. Mater. Interfaces*, 2011, **3**, 3411–3418.
- 9 (a) Y. Q. Dong, J. W. Y. Lam, A. J. Qin, J. Z. Liu, Z. Li and B. Z. Tang, *Appl. Phys. Lett.*, 2007, **91**, 011111; (b) Y. Q. Dong, J. W. Y. Lam, A. J. Qin, Z. Li, J. Z. Liu, J. Z. Sun, Y. P. Dong and B. Z. Tang, *Chem. Phys. Lett.*, 2007, **446**, 124–127; (c) Z. Li, Y. Q. Dong, J. W. Y. Lam, J. X. Sun, A. J. Qin, M. Haubler, Y. P. Dong, H. H. Y. Sung, I. D. Williams, H. S. Kwok and B. Z. Tang, *Adv. Funct. Mater.*, 2009, **19**, 905–917; (d) H. Tong, Y. N. Hong, Y. Q. Dong, M. Haubler, Z. Li, J. W. Y. Lam, Y. P. Dong, H. H. Y. Sung, I. D. Williams and B. Z. Tang, *J. Phys. Chem. B*, 2007, **111**, 11817–11823; (e) C. P. Y. Chan, M. Haubler, B. Z. Tang, Y. Q. Dong, K. K. Sin, W. C. Mak, D. Trau, M. Seydack and R. Renneberg, *J. Immunol. Methods*, 2004, **295**, 111–118; (f) Y. N. Hong, M. Haubler, J. W. Y. Lam, Z. Li, K. K. Sin, Y. Q. Dong, H. Tong, J. Z. Liu, A. J. Qin, R. Renneberg and B. Z. Tang, *Chem.–Eur. J.*, 2008, **14**, 6428–6437; (g) P. Lu, J. W. Y. Lam, J. Z. Liu, C. K. W. Jim, W. Z. Yuan, N. Xie, Y. C. Zhong, Q. Hu, K. S. Wong, K. K. L. Cheuk and B. Z. Tang, *Macromol. Rapid Commun.*, 2010, **31**, 834–839; (h) J. Wang, J. Mei, W. Z. Yuan, P. Lu, A. J. Qin, J. Z. Sun, Y. G. Ma and B. Z. Tang, *J. Mater. Chem.*, 2011, **21**, 4056–4059.
- 10 (a) X. Feng, B. Tong, J. B. Shen, J. B. Shi, T. Y. Han, L. Chen, J. G. Zhi, P. Lu, Y. G. Ma and Y. P. Dong, *J. Phys. Chem. B*, 2010, **114**, 16731–16736; (b) T. Y. Han, X. Feng, B. Tong, J. B. Shi, L. Chen, J. G. Zhi and Y. P. Dong, *Chem. Commun.*, 2012, **48**, 416–418.
- 11 (a) X. Luo, S. Wu and Y. Liang, *Chem. Commun.*, 2002, 492–493; (b) M. Apostol, P. Baret, G. Serratrice, J. Desbrières, J.-L. Putaux, M.-J. Stébé, D. Expert and J.-L. Pierre, *Angew. Chem., Int. Ed.*, 2005, **44**, 2580–2582.
- 12 (a) T. Owen and A. Butler, *Coord. Chem. Rev.*, 2011, **255**, 678–687; (b) T. Owen, R. Pynn, J. S. Martinez and A. Butler, *Langmuir*, 2005, **21**, 12109–12114; (c) F. Molina, C. Llacer, A. O. Vila, A. Puchol and J. Figueruelo, *Colloids Surf., A*, 1998, **140**, 91–101.
- 13 (a) C. Lapouge and J. P. Cornard, *ChemPhysChem*, 2007, **8**, 473–479; (b) J. P. Cornard, A. Caudron and J. C. Merlin, *Polyhedron*, 2006, **25**, 2215–2222.